

**Oiva gold-quartz dyke in the Lapland granulite belt,
Laanila, northern Finland: Case study on high-voltage selective
fragmentation for detailed mineralogical and analytical investigation**

GEOLOGIAN TUTKIMUSKESKUS

Tutkimusraportti 193

GEOLOGICAL SURVEY OF FINLAND

Report of Investigation 193

Tegist Chernet

**OIVA GOLD-QUARTZ DYKE IN THE LAPLAND GRANULITE BELT, LAANILA,
NORTHERN FINLAND: CASE STUDY ON HIGH-VOLTAGE SELECTIVE
FRAGMENTATION FOR DETAILED MINERALOGICAL AND ANALYTICAL
INVESTIGATION**

Unless otherwise indicated, the figures have been prepared by the author of the publication.

Layout: Elvi Turtiainen Oy

Espoo 2011

Chernet, T. 2011. Oiva gold-quartz dyke in the Lapland granulite belt, Laanila, northern Finland: Case study on high-voltage selective fragmentation for detailed mineralogical and analytical investigation. *Geological Survey of Finland, Report of Investigation 193*, 16 pages, 23 figures and 4 tables.

A short-pulsed high-voltage selective fragmentation test was performed on samples from the Oiva gold-quartz dyke to liberate gold and related minerals using selFrag laboratory scale equipment. SelFrag was able to release individual grains of gold, electrum and other minerals of interest, preserving their original texture, shape and size, and provided an opportunity for detailed study of their morphology, surficial features, grain size and composition.

The mineralogy of gold/electrum and associated ore minerals was studied by light and electron microscopy using various non-magnetic, heavy mineral concentrates (<200 µm and 2 mm–200 µm) of the fragmented samples. As a result, a number of gold/electrum grains were recovered from fragmented and preconcentrated samples. The composition of gold/electrum varied from about 27.15 to 96.06 wt% Au and from 3.5 to 72.85 wt% Ag, with an Ag/Au ratio of 0.04–2.68. Morphologically, gold/electrum grains were irregular, globular, branched, grooved, subrounded, flaky, and commonly <50 µm in size. Although chalcopyrite was relatively common, other sulphides were generally fine grained, disseminated and rare. Gold/electrum was goethite-quartz hosted and infrequently associated with silver telluride, bismuth telluride, native bismuth, Ag sulphide and Ag halide.

Based on mineralogical evidence, the primary electrum might have been deposited with chalcopyrite and other base metal sulphides, and partially remobilized by either late-stage hydrothermal fluid or supergene processes for the depletion of its silver to form fine-grained native gold. Such secondary enrichment might also be supported by the presence of secondary acanthite, iodyrite and covellite, which might only be possible to recover using selective fragmentation and consecutive preconcentration processes.

Keywords (GeoRef Thesaurus, AGI): gold ores, quartz veins, sample preparation, selective fragmentation, gold, electrum, mineralogy, chemical composition, Laanila, Inari, Finland

*Tegist Chernet
Geological Survey of Finland
P.O. Box 96
FI-02151 Espoo
Finland*

E-mail: tegist.chernet@gtk.fi

ISBN 978-952-217-176-4 (PDF)
ISSN 0781-4240

Chernet, T. 2011. Oiva gold-quartz dyke in the Lapland granulite belt, Laanila, northern Finland: Case study on high-voltage selective fragmentation for detailed mineralogical and analytical investigation. *Geologian tutkimuskeskus, Tutkimusraportti 193*, 16 sivua, 23 kuvaa ja 4 taulukkoa.

Korkeajännitepulssitusta selFragLab-laitteella kokeiltiin kulta- ja muiden malmimineraalipartikkelien irrottamiseen Oivan kulta-kvartsijuonesta otetuista näytteistä. Talteen saatiin kulta-, elektrumi- ja muita mielenkiintoisia mineraalipartikkeleita niin, että niiden alkuperäinen rakenne, muoto ja koko olivat säilyneet. Näin oli mahdollista tutkia rakeita yksityiskohtaisesti ja selvittää niiden morfologiaa, pintarakenteita, raekokoa ja koostumusta.

Hajotetusta kiviaineksesta preparoitiin magneettisesti ja raskasneusteillä separoituja mineraalikonsentraatteja ($d > 3,3$, $EM < 0,2$ mm ja $0,2-2,0$ mm), joita mikroskojottiin sekä optisesti että elektronioptisesti. Talteen saatiin joukko kulta- ja elektrumpartikkeleita, joiden kultapitoisuus oli $27,15-96,06\%$ ja hopeapitoisuus $3,5-72,85\%$ ja joiden Ag/Au -suhde vaihteli $0,04\%$:sta $2,68\%$:iin. Rakeet olivat morfologialtaan epäsäännöllisiä, pallomaisia, haarauneita tai kuoppaisia, levymäisiä tai jonkin verran pyörityneitä sekä läpimitaltaan yleisesti < 50 μm . Huolimatta kuparikiisun yleisyydestä muita sulfidimineraaleja esiintyi vain vähän ja hienorakeisena piroteena. Kulta/elektrumi esiintyi kvartsigötiitissä ja joskus myös Ag -telluridien, Bi -telluridien ja vismutin sekä Ag -sulfidien ja -halidin yhteydessä.

Havaintojen perusteella primääri elektrumi saattaisi liittyä kuparikiisun ja muiden metallisulfidien kiteytymiseen, mutta osaksi se remobilisoitui myöhäisissä hydrotermisissä tai pintaprosesseissa. Tällöin hopeapitoisuus väheni, ja samalla kiteytyi hienorakeisia kultapartikkeleita. Ajatusta sekundäärisestä rikastumisesta tukee sekundäärisen acantiitin, hopeajodidin ja kovelliitin esiintyminen. Saattaa olla, että näiden mineraalien esiintymistä ei olisi lainkaan havaittu ilman korkeajännitepulssituksella aikaansaattua selektiivisyyttä kiven sisältämien mineraalipartikkelien vapautumisessa.

Asiasanat (Geosanasto, GTK): kultamalmit, kvartsijuonet, näytteen käsittely, selektiivinen fragmentointi, kulta, elektrumi, mineralogia, kemiallinen koostumus, Laanila, Inari, Suomi

Tegist Chernet
Geologian tutkimuskeskus
PL 96
02151 Espoo

Sähköposti: tegist.chernet@gtk.fi

CONTENTS

1 INTRODUCTION.....	5
2 SELECTIVE FRAGMENTATION.....	7
3 MATERIALS AND METHODS.....	7
4 RESULTS.....	8
4.1 Heavy mineral concentrates.....	8
4.2 Polished thin sections and heavy mineral grains.....	9
4.3 Composition, shape and grain size distributions of gold/electrum grains.....	13
5 DISCUSSION.....	14
6 SUMMARY AND CONCLUSIONS.....	15
7 ACKNOWLEDGEMENTS.....	16
REFERENCES.....	16

1 INTRODUCTION

Along with a number of other deposits, the Oiva gold-quartz dyke, which is situated together with the Laanila diabase in the northeastern shear zone near Inari in Finnish Lapland, has boosted gold exploration in the Laanila area (Fig. 1). The Laanila target area belongs to the Palaeoproterozoic granulite belt (Keinänen et al. 2010). The Oiva dyke is named after a geology student, Oiva Varjos, who collected and submitted samples to the Geological Survey of Finland (GTK) for chemical analysis. The samples found to be mineralized with gold, silver and copper. Some of the collected stone- to cobble-size pieces of quartz vein have been documented, for instance by Keinänen et al. (2010) (Fig. 2).

Short-pulsed high-voltage selective fragmentation to liberate gold and related minerals for applied and process mineralogical studies has major advantages compared to conventional mechanical crushing and grinding. A number of authors have documented comparative particle liberation test results. For example, the disintegration of an oxide ore containing hematite, PGMs, complex Cu sulphides and pentlandite by electric pulses generated a higher percentage of liberated mineral particles and a lower percentage of fines than obtained by mechanical comminution (Andres et al. 2000). A comparative liberation study on Merensky reef samples using electric pulse disaggregation and mechanical crushing indicated higher liberation of chromite, pentlandite, pyrrhotite and PGM than that obtained using a jaw crusher (Lastra & Cabri 2003). Selective fragmentation (selFrag) and a roller crusher have been compared as methods to liberate and recover kimberlite/diamond indicator minerals from kimberlite rock pieces, and zircon, titanite, beddeleyite,

monazite and apatite from tonalite and diabase rocks (Chernet 2006, Chernet 2007, Chernet et al. 2007). There were strong indications that selFrag generate better liberation of such accessory minerals than the roller crusher.

Fragmentation and grain separation primarily occurs along grain boundaries, with superior preservation of the original grain size and shape, and hence allows far greater recovery. Concentrates of liberated and unaffected mineral grains yield ample mineralogical information. Further advantages of high-voltage selective fragmentation technology include simplified sample processing, reduced use of human resources, reduced energy consumption and a lower risk of contamination.

Recently, the Geological Survey of Finland (GTK) installed selFrag equipment for electrical comminution at the laboratory scale at its premises in Espoo. The GTK Research Laboratory is developing its application for the liberation and recovery of particular mineral fractions suitable for isotope geochemistry as well as for mineral processing and exploration studies on diamond, gold, PGE and other precious and base metals. The main objectives of these latter studies include:

1. to assess the performance of electrical fragmentation in preserving mineral grain size and shape, texture, alteration rims and other surface features, to be able to extract more detailed information on the formation and deposition of the gold, and
2. to identify gold and associated minerals, and to determine the distribution, grain size, proportion and intergrowth with the mineral assemblages in the rock samples from the Oiva gold-quartz dyke and associated rocks.

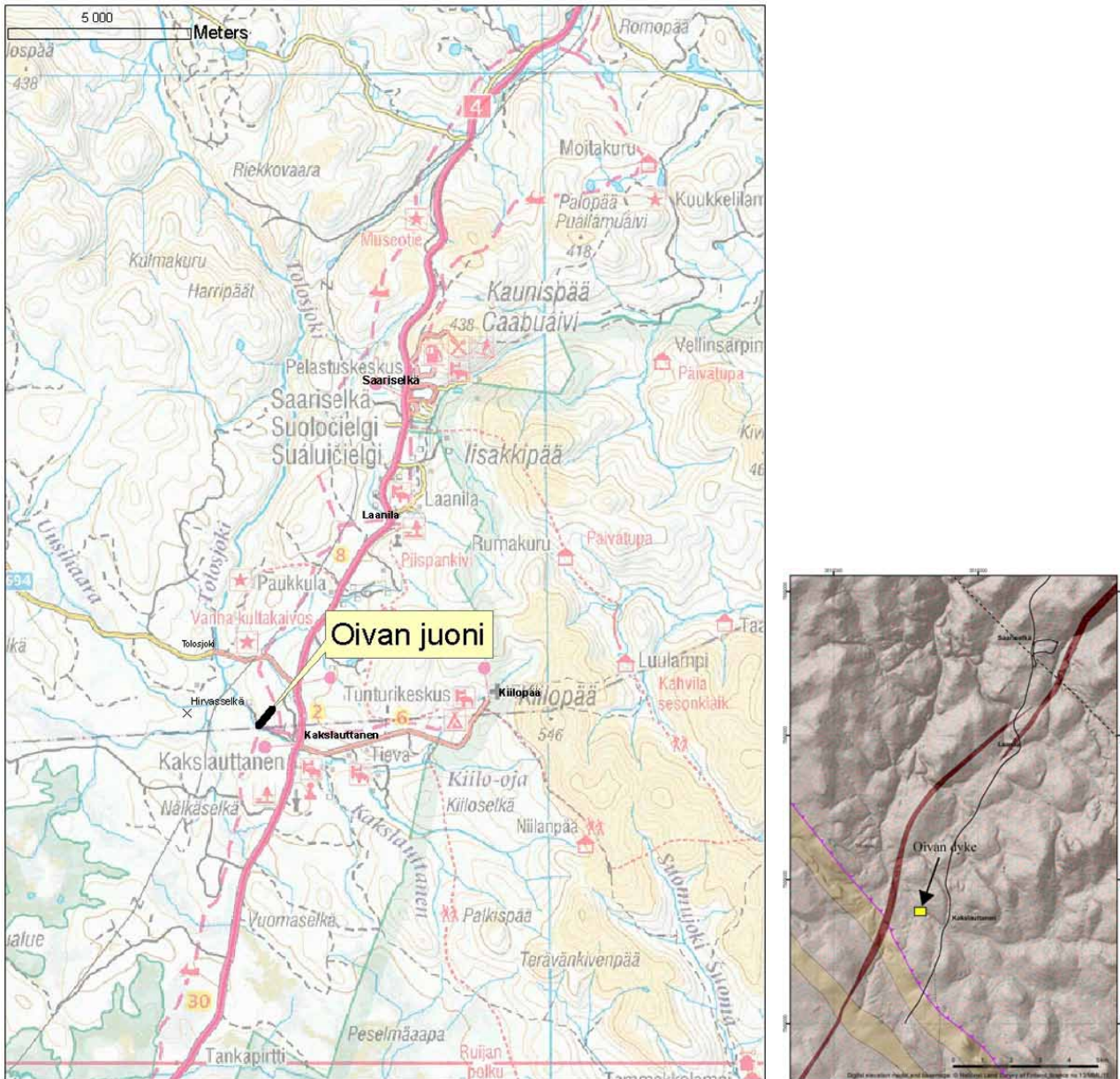


Fig.1. Map showing the location of the Oiva gold-quartz dyke, and bedrock map of Laanila (GTK): Laanila diabase (dark brown), garnet-gneiss and hyperstene-quartz-diorite (light brown) in the granulite belt (from Keinänen et al. 2010).



Fig. 2. Stone- to cobble-sized pieces of quartz vein from the Oiva dyke; length of plate 10 cm (Keinänen et al. 2010).

2 SELECTIVE FRAGMENTATION

Selective fragmentation using selFrag is a laboratory-scale comminution technology by which mineral grains are liberated from morphologically intact rocks, mineral aggregates and/or geological composite materials without being damaged or broken (Fig. 3). Unlike conventional comminution equipment (e.g., jaw-, gyratory-, roller-crushers), which causes particle breakage under compression or impact loading, selFrag applies a high-voltage electrical discharge that induces tensional stress in the rock, leading to disaggregation of mineral grains. The high-voltage electrical discharge results in short-lived plasma that is agitated as a shock wave in rock, preferentially along weak zones such as grain boundaries, pre-existing fractures and discontinuities in a crystal lattice. As a result, individual mineral grains are released, retaining their natural size and shape, facilitating the assessment of grain dimensions, morphology,

crystal structure, physical and textural features, and chemical compositions.

Several authors (e.g., Andres 1995, Bluhm et al. 2000, Gnos et al. 2007, Cabri et al. 2008) have described the general principle of operation for high-voltage fragmentation. The application of high-voltage discharge pulse disaggregation is a novel sample processing technique for gold mineralogy. Cabri et al. (2008) published a promising report on electric pulse disaggregation (EPD) by CNT Spark-2 in the process mineralogy of precious metals and related ore types.

SelFrag equipment is produced by the Swiss company selFrag AG, which was spun off from Ammann Group in 2008. The equipment has now been installed in a few research laboratories and universities and is suitable for batch processing of limited-sized samples for specific applications.

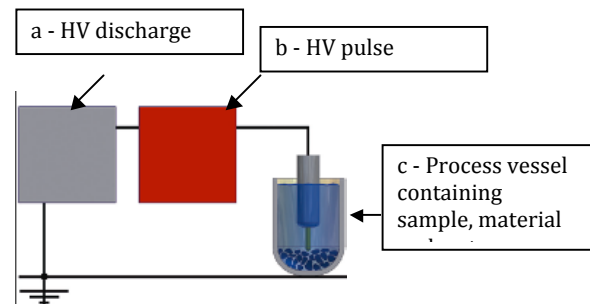


Fig. 3. SelFrag equipment and its main components: a – HV discharge, b – HV pulse, c – Process vessel containing sample, material and water.

3 MATERIALS AND METHODS

The materials investigated here comprised hard rock samples extracted from different zones in the Oiva dyke, both with and without gold mineralization. The samples were collected for assessment of their mineral content and other properties based on gold assay results (Table 1), which demonstrated a considerable geochemical correlation between Au and the concentrations of Ag, Bi, Te, Fe, Cu and S.

Polished thin sections were prepared from each sample using standard procedures (see e.g. Grondijs & Schouten 1931, Hutchinson 1974, and Humphries 1992) to assess the mineral content as well as the textural and structural relationships. The remaining material was comminuted by electrical pulse disaggregation using selFrag equipment. Polished sections were initially studied with a Leica petrographic microscope in transmitted

Table 1. Geochemical analysis of bulk rock samples by ICP-MS and ICP-AES, in ppm, Au in ppb.

Sample no.	Sb	Bi	Te	Ag	Al	As	Ba	Ca	Cr	Cu	Fe	K	Mg
OS-08-4.1	<0.02	0.03	0.01	1	29300	<10	52	107	73	315	57300	1360	18200
OS-08-4.2	0.06	9.07	4.12	108	882	<10	16	84	58	9390	173000	<200	73
OS-08-4.3	0.04	7.50	3.98	50	296	17	15	109	16	4650	94800	<200	<50
OS-08-4.4	<0.02	1.70	1.30	<1	15500	<10	41	91	33	2040	39400	1240	6570
OS-08-4.6	0.03	7.06	3.51	114	536	<10	15	96	24	10300	114000	<200	<50
OS-08-4.9	0.04	10.30	7.72	43	402	322	15	88	22	4490	148000	<200	65

Sample no.	Mn	Mo	Na	Ni	P	S	Sc	Ti	V	Y	Zn	Au
OS-08-4.1	120	<2	293	19	<50	<20	5.7	53	66	6.6	12	16
OS-08-4.2	<1	10	276	<3	128	683	<0.5	6	15	1.0	21	19300
OS-08-4.3	<1	4	273	<3	<50	1560	<0.5	4	6	<0.5	13	21000
OS-08-4.4	61	<2	237	10	90	<20	2.2	32	24	6.1	15	55
OS-08-4.6	<1	4	295	<3	<50	2870	<0.5	5	9	<0.5	24	29200
OS-08-4.9	<1	4	242	<3	<50	3770	3.6	41	34	3.2	15	14900

Note: B < 5, Cd < 1, Co < 5, Sr < 5, Be < 0.5, Pd < 10, Pb < 10

and incident illumination. For gold and related metals beyond optical resolution, polished sections were sputter-coated with carbon. The carbon-coated sections were examined using a Jeol JMS 5900LV SEM-EDS instrument to assess the grain morphology and composition. INCA Feature software by Oxford Instruments was used for automatic searching and classifying of gold and other related phases. INCA Feature uses a back-scattered electron image (BSE) (or SE image for shape classifications) to separate the phases. These phases are subsequently analysed with fast EDS analysis (2–5 s) with the accelerating voltage set at 20 kV and an electron probe current of 1–2 nA, and are then classified.

Micrographs were recorded in BSE imaging modes. To determine the chemical composition, selected mineral grains were analysed by EDS at 20 kV and 10 nA with a 60 s acquisition time and 30% dead time. The same instrument settings and operating conditions were applied for the study of comminuted materials described below.

Representative samples that were hammered to rock chips of 3 to 4 cm in size were prepared for fragmentation. Four samples (200–400 g each) were fragmented and further classified into three grain size classes (>2 mm, 2 mm–200 µm, <200 µm). Fractions >2 mm were studied without further preparation under a Leica MZ APO stereomicroscope with an attached Leica DC 300 digital microscope camera + LAS version 2.8.1 software. Fractions of 2 mm–200 µm and <200 µm were refined by heavy media separation (HMS), and heavy fractions ($d > 3.3 \text{ g}\cdot\text{cm}^{-3}$) further separated by a Frantz electromagnetic separator using standard procedures of the GTK Research Laboratory. Non-magnetic concentrates from 2 mm–200 µm fractions were studied under a stereomicroscope, and gold and heavy mineral grains were handpicked for detailed assessment by SEM-EDS. Non-magnetic concentrates from <200 µm fractions were carefully prepared using carbon tape for studies by SEM-EDS.

4 RESULTS

4.1 Heavy mineral concentrates

Microscope observation revealed that gold and related minerals down to a few micrometres in size were released and recovered, preserving their shape, size and surface morphology as in the

original rock material. Table 2 presents the results of fragmentation, screening, HMS, magnetic separation and recovery of gold from the two main fractions. Interestingly, recovery from the

Table 2. Recovery of gold/electrum from selected samples by selFrag comminution and subsequent processing.

Sample no.	Total weight (g)	Sieve fractions (g)			HMS heavy fraction $d > 3.3$ (g)	
		>2 mm	2 mm–200 μm	<200 μm	2 mm–200 μm	<200 μm
OS-08-4.9	212	3.6	117.3	84.6	20.8	33
OS-08-4.2	417.5	50	261.2	99.6	10.8	22.5
OS-08-4.2a	354.5	42	232.2	73.8	1.71	4.9
OS-08-4.3a	240	8.8	141.1	83.3	7.9	22.5
Sample no.	HMS heavy fraction ($d > 3.3$) and non-magnetic (after Frantz 0.6 A) (g)		Gold grains recovery (non-magnetic fractions)			
	2 mm–200 μm , non-magn. (0.6 A)	<200 μm , non-magn. (0.6 A)	2 mm–200 μm , picked (grains)	<200 μm , SEM-feature detected gold/electrum (grains)		
OS-08-4.9	0.13	0.12	1	>850		
OS-08-4.2	0.05	0.07	11	>3700		
OS-08-4.2a	0.22	0.09	5	>2000		
OS-08-4.3a	0.2	0.12	0	>400		

coarse fraction (2 mm–200 μm) correlated well with recovery from the finer fraction (<200 μm). Furthermore, the weights of fragmented samples

were positively correlated with the recovery of gold, implying that the distribution of gold in all samples was similar.

4.2 Polished thin sections and heavy mineral grains

The predominant secondary mineral in the Oiva dyke directly related to its gold mineralization was determined to be goethite, lining and/or filling cracks in quartz grains forming dendritic structures, and constituting 5–10 vol% of the bulk rock (Figs. 4–5). Fine-grained chalcopyrite and rutile were usually associated with goethite and en-

closed in large grains of quartz and quartz aggregates. Primary minerals of arsenopyrite, pyrite, cobaltite, galena and sphalerite were infrequently observed along with the relatively common mineral, chalcopyrite. Replacement of chalcopyrite with covellite and secondary iron oxide was observed in the rock (Fig. 6).

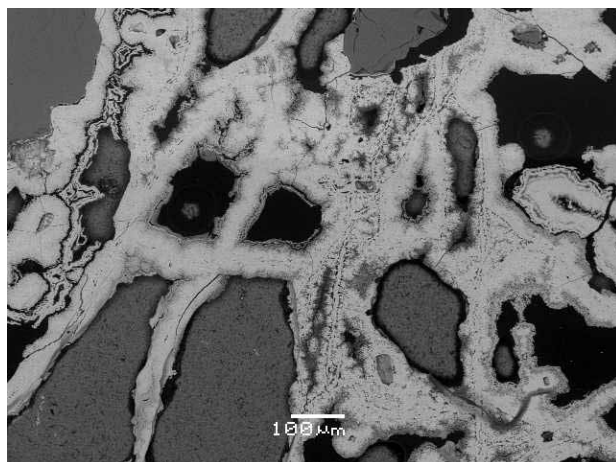


Fig. 4. Goethite mass filling fractures and cavities mainly in quartz (BSE image, OS-08-4.6).

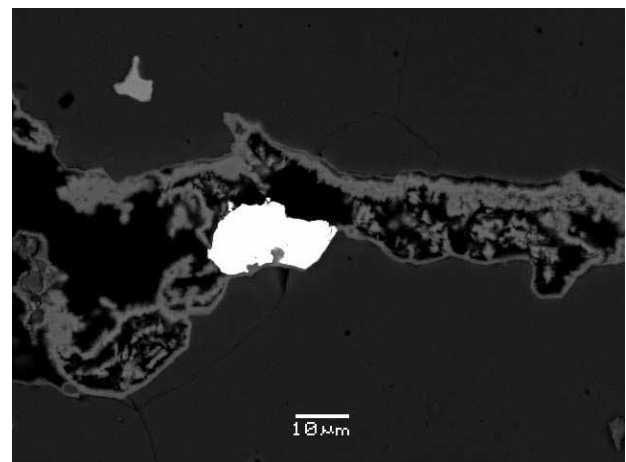


Fig. 5. Electrum (Au = 58.4 wt%, Ag = 39.8wt%) associated with goethite that fills openings and fractures in quartz (BSE image, OS-08-4.6).

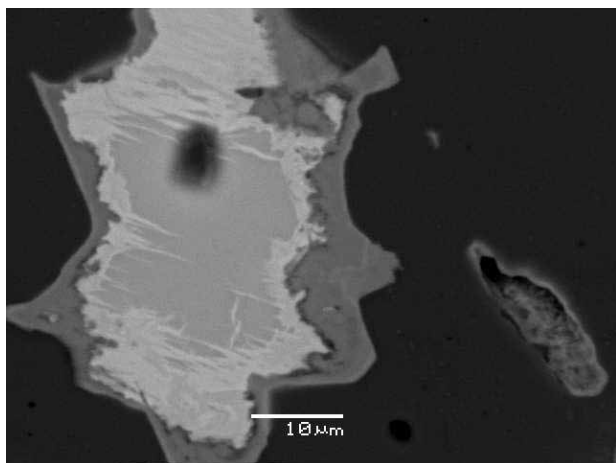


Fig. 6. Replacement of chalcopyrite by covellite, and covellite rimmed by goethite (LM image OS-08-4.6).

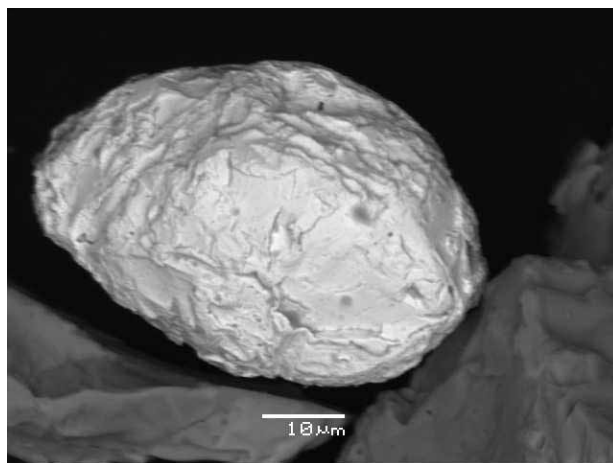


Fig. 7. Liberated, massive/subrounded native gold (Au = 90–92 wt%, Ag = 7–9 wt%) (BSE image OS-08-4.0).

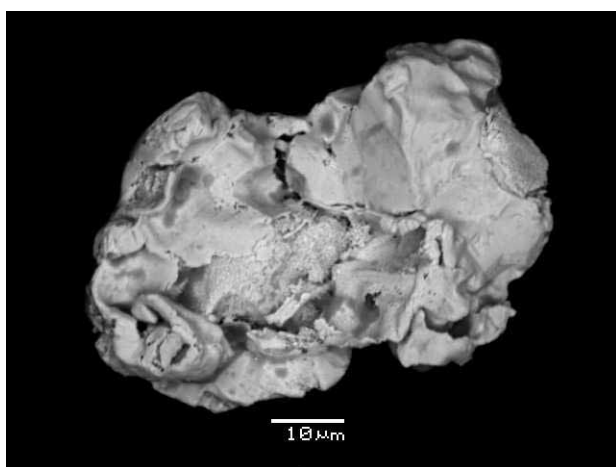


Fig. 8. Native porous gold grain (core, Au = 83.9–96 wt%, Ag = 3.9–7.6 wt%) with electrum rim (outer, Au = 54.6–63.8 wt%, Ag = 36.2–45.7 wt%) (BSE image, OS-08-4.2a).

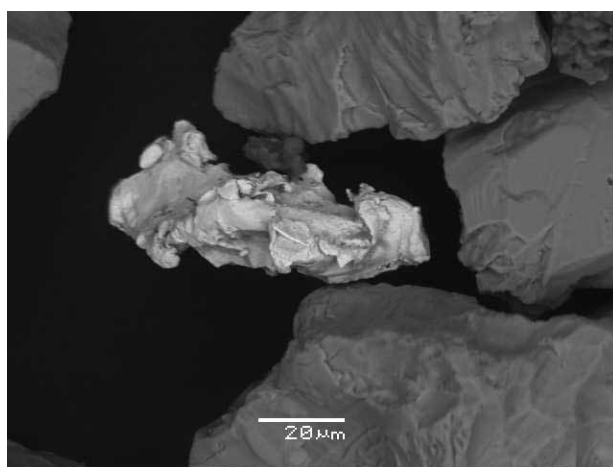


Fig. 9. Electrum with a higher silver content (points 3 & 4 – Au = 52.8 wt%, Ag = 47.2 wt%) and lower silver content (points 1 & 2 – Au = 88–90.3 wt%, Ag = 3.5–5.4 wt%) (BSE image, OS-08-4.2a).

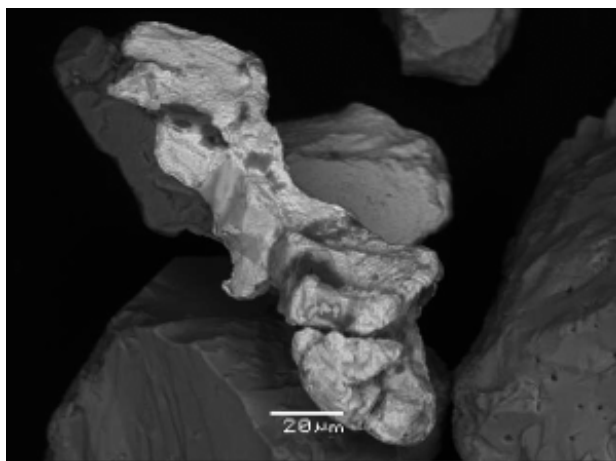


Fig. 10. Native gold composition as part of electrum (points 1 & 2 – Au = 93.7 wt%, Ag = 6.3 wt%); note the porous structure of the gold (BSE image, OS-08-4.2).

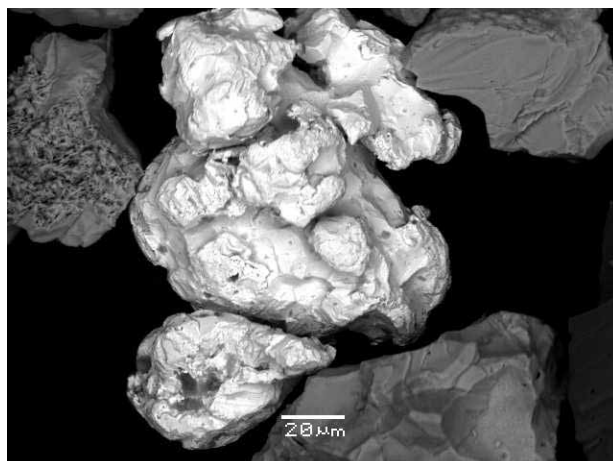


Fig. 11. Electrum (Au = 49.4–62.8 wt%, Ag = 30.0–50.6 wt%) with a botryoidal/globular structure (BSE image, OS-08-4.2).

Less common components included disseminated native gold (Figs. 7–8), electrum (Figs. 8–13), acanthite (Ag_2S), iodargyrite (AgI), silver telluride, bismuth telluride and metallic bismuth. Gold and electrum often occurred as small grains ($<50\ \mu\text{m}$) on the goethite surface or embedded in open spaces between goethite or along the boundaries between quartz and goethite (Fig. 5). The cavities of relatively larger electrum grains were filled with secondary Fe-oxides or altered magnetite and rutile relics. Native gold ($\text{Au} = 80\text{--}99\ \text{wt}\%$) was scarce, and occurred in three forms, notably as:

1. rounded separate grains (Fig. 7),
2. a porous gold-rich core with a silver-rich rim (Figs. 8 and 9), and
3. a randomly distributed porous gold-rich part of electrum (Fig. 10).

Some electrum grains had a porous, gold-rich core and outer part, which was observed under

SEM-EDS from unaffected liberated grains fastened onto tape (Figs. 8, 9 and 10). Most of the gold, however, occurred as electrum with a variable amount of $\text{Ag} > 20\ \text{wt}\%$ (Figs. 9–13).

The presence of native silver was not clear because of an overlapping fine-grained ($<5\ \mu\text{m}$) acanthite composition with a variable sulphur content associated with goethite. The silver mineral assemblage was dominated by acanthite (Ag_2S ; Figs. 14–16) and iodargyrite (AgI ; Fig. 17), which occurred in association with goethite and quartz grains as cavity- and fracture-filling structures. Acanthite was found as a thin layer covering chalcopryrite and silver-rich electrum (Fig. 15), a rhythmic banding texture with goethite (Fig. 16) and as individual anhedral grains that often displayed twinning (Fig. 14). In contrast, fine-grained iodargyrite often appeared in well-developed crystals associated with electrum, goethite, chalcopryrite and quartz. Isolated grains of silver

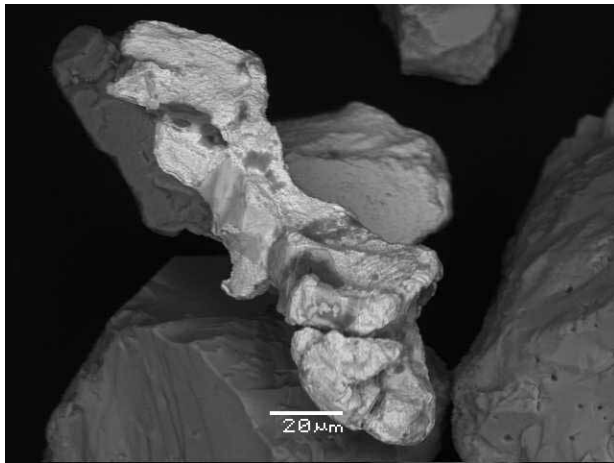


Fig. 12. Dendritic/ branched electrum ($\text{Au} = 44.5\text{--}66\ \text{wt}\%$, $\text{Ag} = 29.5\text{--}43.4\ \text{wt}\%$) (BSE image, OS-08-4.0).

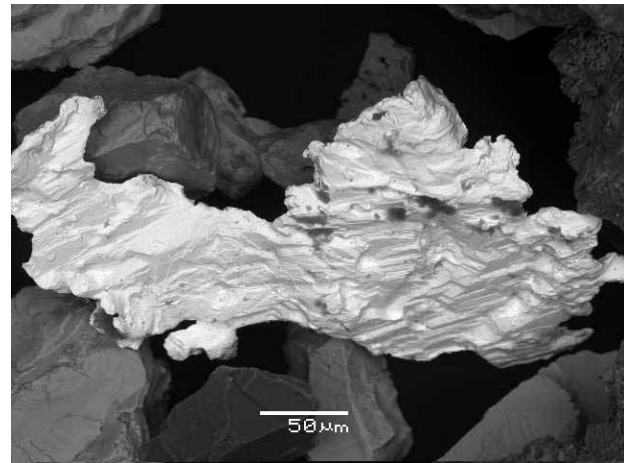


Fig. 13. Flaky electrum ($\text{Au} = 50.6\text{--}52\ \text{wt}\%$, $\text{Ag} = 48\text{--}49.5\ \text{wt}\%$) showing a striated crystal surface (BSE image, OS-08-4.2).

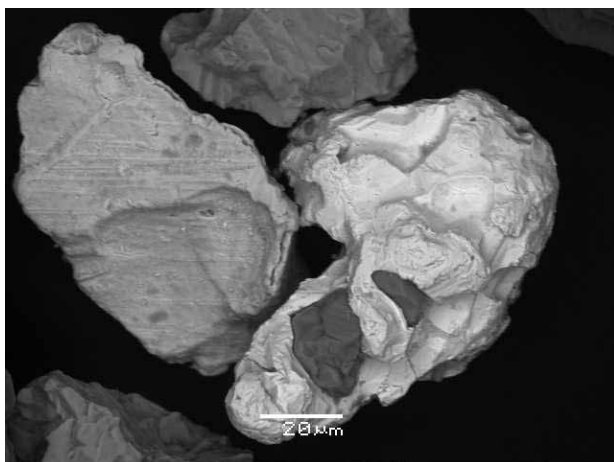


Fig. 14. Acanthite (light grey, $\text{Ag} = 85\text{--}87\ \text{wt}\%$, $\text{S} = 13\text{--}15\ \text{wt}\%$) and electrum (light) with embedded Fe-oxide grains (BSE image, OS-08-4.2).

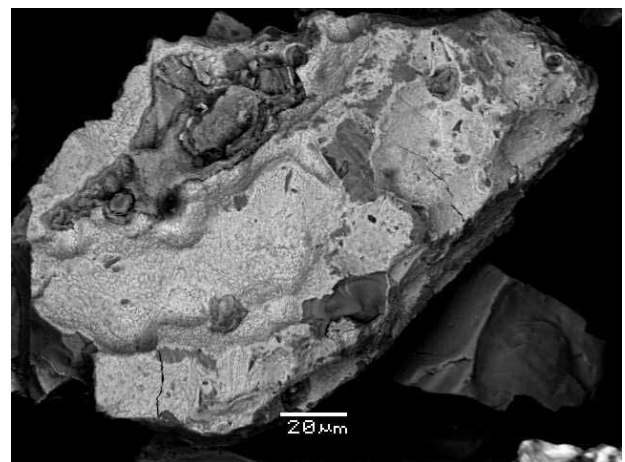


Fig. 15. Silver sulphide (acanthite) ($\text{Ag} = 62\text{--}74\ \text{wt}\%$, $\text{S} = 25\text{--}37\ \text{wt}\%$) developed on the surface of chalcopryrite (BSE image, OS-08-4.0).

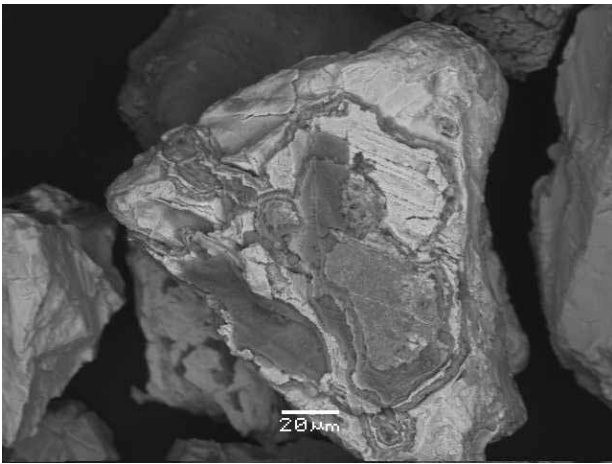


Fig. 16. Acanthite (Ag = 76–88 wt%, S = 11–23 wt%) intergrown with goethite (BSE image, OS-08-4.2).

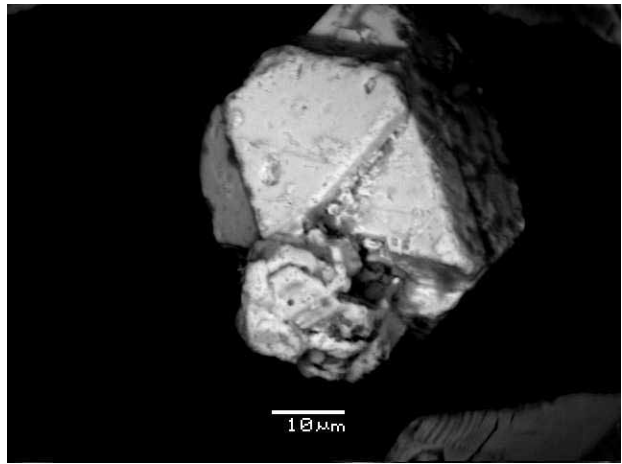


Fig. 17. Well-developed crystal of iodargyrite (AgI) (Ag = 49.7–54 wt%, I = 45.9–50.2 wt%) (BSE image, OS-08-4.0).

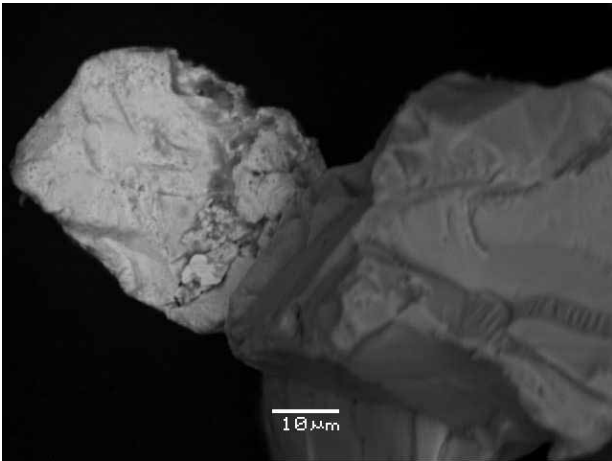


Fig. 18. Silver telluride (40 μm across) (Ag = 63.9–64.6 wt%, Te = 35.4–36.5 wt%) (BSE image, OS-08-4.0).

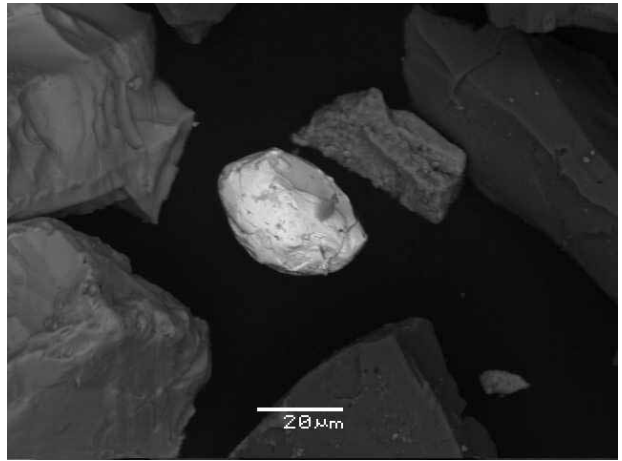


Fig. 19. Bismuth telluride (bright grain, 25 μm across) (Bi = 57.2 wt%, Te = 42.7 wt%) (BSE image, OS-08-4.0).

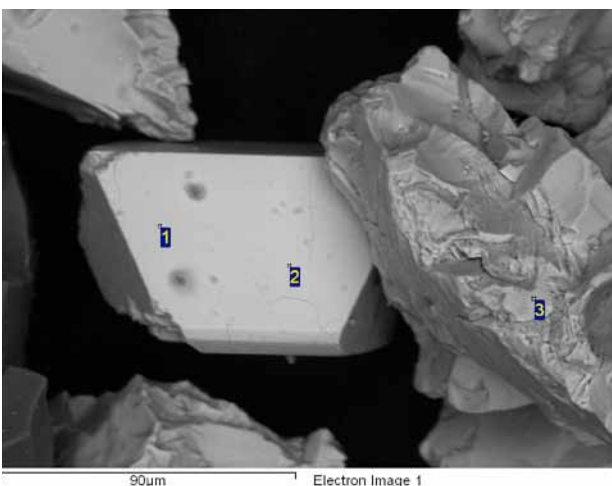


Fig. 20. Well-developed euhedral crystal of cobaltite (CoAsS) (BSE image, OS-08-4.3a).

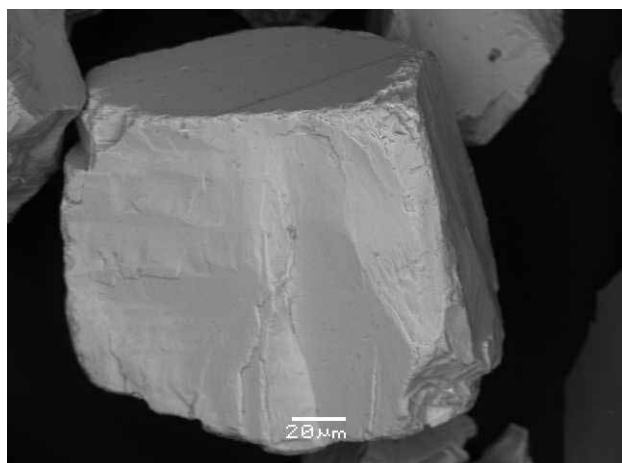


Fig. 21. Barite grain with a perfect crystal shape (BSE image, OS-08-4.2a).

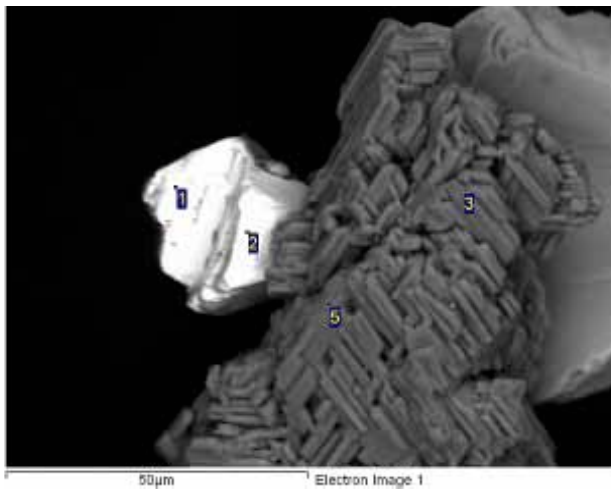


Fig. 22. Small crystal of galena (bright) with extensively twinned rutile (BSE image, OS-08-4.2a).

telluride (hessite) (Fig. 18), bismuth telluride (tellurobismuthite) (Fig. 19) and native bismuth (Bi) were observed in association with electrum, chalcopyrite, galena and cobaltite. Other rare minerals that occurred disseminated within quartz-goethite rock include barite (BaSO_4), molybdenite (MoS_2) and complex assemblages, which were enriched in U, Th and Pb. Most of the heavy mineral grains described here were liberated free grains with their original texture, shape, size and crystal

4.3 Composition, shape and grain size distributions of gold/electrum grains

Hundreds of liberated gold/electrum grains were analysed with SEM to determine the gold and silver content. Pure native gold is defined as containing less than 20 wt% of Ag and pure native silver has less than 20 wt% of Au, with intermediate compositions determined as electrum. The presence of other impurities may render the Au content in pure gold (and conversely, the Ag content in pure silver) less than 80 wt%. Gold/electrum in the present samples was strictly associated with goethite and quartz, and ranged in composition from 27–96 wt% Au to 4–73 wt% Ag. Only a few analysis points showing Ag > 80 wt% were recorded. The semi-quantitative measurements revealed chemical variability in each gold/electrum grain. The Ag/Au ratio from each sample is presented in Table 3. These ratios indicate that native gold and silver-rich electrum were present in most of the samples, whereas pure native silver with <20 wt% Au was very rare or absent.

The data collated in Table 3 are plotted graphically in Figure 23. Compositions ranging from ‘pure gold’ to ‘pure silver’ and intermediate elec-

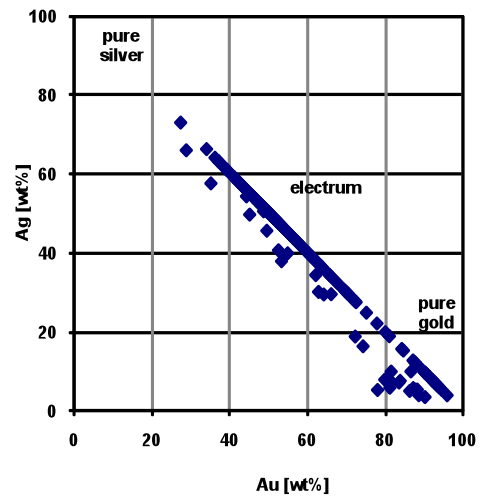


Fig. 23. Ag-Au proportions in wt% determined by SEM-EDS in gold and electrum grains from the Oiva dyke (>300 analyses).

structure well preserved. Well-developed euhedral crystals of cobaltite, barite, galena and rutile were documented (Figs. 20–22).

Gangue minerals were dominated by quartz with minor amounts of feldspar, mica and carbonates. Samples submitted from the surrounding altered granulite were dominated by mica (mainly chloritic), Na and K feldspars and quartz, with minor amounts of rutile, zircon, monazite and xenotime (OS-08-4.1 and OS-08-4.4 in Table 1).

trium are plotted on the diagonal from 100 wt% Au to 100 wt% Ag. A few analysed grains were classified as pure gold, none as pure silver, and most as electrum, but the compositional range of electrum was three times wider. Data points plotting below the diagonal imply the presence of impurities, mainly Fe, Cu and Hg, reducing the sum of Au+Ag to <100 wt%. The gold grains handpicked from the coarser fraction (2 mm–200 µm) were all composed of electrum (Au = 29–71 wt%, Ag = 30–66 wt%), clearly implying that pure gold grains were finer than electrum grains. Gold and electrum grains in the fine fraction (<200 µm) showed a wide range in composition. Grains of pure gold with Au = 80–96 wt% and Ag = 3–20 wt% were restricted to the fine fractions as separate grains and were associated with electrum.

Individual gold/electrum grains were observed to have variable shapes, such as branched (or dendritic), irregular, massive, subrounded, grooved, botryoidal or globular, and could also be sponge-like without any crystal faces (Figs. 7–13). Separate pure gold grains were often mas-

Table 3. Ag/Au ratio from over 300 analyses (SEM-EDS).

Sample	Ag/Au	
	Min	Max
OS-08-4.0	0.07	1.95
OS-08-4.2	0.07	1.40
OS-08-4.2a	0.04	2.68
OS-08-4.3a	0.41	1.64

Table 4. Size distribution of gold and electrum grains by SEM-BSE from the <200 µm fraction in sample OS-08-4.0. Note: Au_low represents a relatively low content of gold due to trace elements and entrapped spectrum from the surroundings.

Class	<25	25-50	50-75	75-100	100-125	125-150	150-175	175-200	≥200
Electrum	201	88	35	10	6	5	3	0	1
Au	143	82	42	13	5	1	0	1	0
Au_low	133	39	16	2	4	0	0	0	0
Ccp	123	44	11	2	1	1	1	0	0
Unclassified	92	18	6	0	0	0	0	0	0
Ag ₂ S	78	5	0	0	1	0	0	0	0
Ag-rich electrum	19	7	3	0	1	0	0	0	0
AgI	21	5	1	0	0	0	0	0	0
AgTe	0	2	0	0	0	0	0	0	0
BiTe	0	2	0	0	0	0	0	0	0

sive and subrounded with rough surfaces (Fig. 7). Electrum was rather irregular, branched, flaky and globular. Flaky electrum was encountered with crystal faces reserved (Fig. 13). Grooved surfaces were filled with entrapped goethite, altered magnetite and/or rutile.

The size distribution of gold and electrum grains in <200 µm fractions as determined using

INCA Feature software from SEM-BSE images is collated in Table 4. The data indicate that most gold and electrum grains were concentrated in fractions <75 µm. This size distribution correlates with the intact rock, demonstrating that the electrical comminution process had indeed preserved the natural grain size.

5 DISCUSSION

Electrum, gold, acanthite and iodargyrite were examined from the partially oxidized and brecciated quartz-rich Oiva dyke. Cavities and fractures between quartz grains were observed to be typically filled or lined by goethite, an Fe-oxide of secondary origin. Gold and electrum mineralization was confined to goethite-quartz veins and associated with assemblages of secondary minerals (e.g., acanthite, iodargyrite and covellite). Goethite hosting electrum in the Morning star deposit in California has been reported to occur as pseudomorphs after pyrite (Sheets et al. 1995). Although no convincing evidence of such a structure was observed in the present samples from the Oiva dyke, fine-grained chalcopyrite (including rarely occurring pyrite and other base metal sulphides) as inclusions in quartz and associated with goethite might be remnants that have persisted complete oxidation.

Several gold/electrum grains with compositions ranging from 27–96 wt% Au and 3–73 wt% Ag were recovered from fragmented and pre-concentrated samples. Gold/electrum was mainly goethite-hosted and deposited along cavities and fractures in quartz grains. Electrum typically occurred in irregular, flaky, branched (dendritic) and globular grains. Grains of pure gold with <20 wt% Ag were rare, often fine grained, massive to subrounded with rough/porous surfaces and associated with electrum. Although native silver was not clearly observed, some grains qualitatively determined as Ag₂S might have been native silver.

Twinning in acanthite has been interpreted as being indicative of inversion from high-temperature polymorph argentite (Sillitoe 2007, Sheets et al. 1995). On the basis of the well-developed form of crystals and abundant twinning, the acanthite at the Oiva dyke might be pseudomorphed crys-

talline argentite (Figs. 14 and 16). On the other hand, a supergene origin could also be indicated by the presence of acanthite as a replacement for pre-existing chalcopyrite (Fig. 15) and electrum. Compositionally, the twinned acanthite was quite pure (Ag = 85–87 wt%, S = 13–15 wt%), and sulphur enrichment could be seen in secondary acanthite (Ag = 62–74wt%, S = 25–37%). Silver halides are typically classified of indicators of arid or semiarid climatic conditions where halides are common in the ground waters (e.g. Boyle 1997, Reich et al. 2009). Iodargyrite from the Chapais region of north-central Quebec was found to be an indicator of a period of preglacial aridity (Boyle 1997). Similarly, along with other climatic indicators, iodargyrite from the Laanila area could be used to confirm the existence of past aridity.

The mineral assemblages and textural relations imply two distinct but continuous stages of Ag–Au mineralization: primary hypogene and secondary, either supergene or late-stage, low-temperature hydrothermal. Ag–Au as electrum and argentite (acanthite at present) might have primarily been deposited with chalcopyrite and other base metal sulphides (arsenopyrite, pyrite, cobaltite, galena and sphalerite). Trace element geochemistry also demonstrated a strong correlation among Au, Ag, Cu, S and Fe (Table 1). The replacement of sulphide minerals may have oc-

curred without affecting the enclosed electrum. The Ag–Au composition as gold/electrum occurs in various textural relationships with goethite and is probably primary. Textural evidence, however, supports late-stage remobilization of at least some of the gold and silver. Deposition/precipitation of fine grains (<20 µm) of gold and electrum on the surface of goethite, variation in the Au composition from the core to the outer surface of electrum grains, and the presence of rim, wire and sponge morphologies in association with acanthite suggest remobilization of some Au and Ag in a late-stage hydrothermal or supergene environment. Additional observations that suggest secondary enrichment at the Oiva dyke include: the presence of secondary acanthite replacing chalcopyrite and the presence of fine-grained iodargyrite; native gold grains being generally finer in size than electrum; the replacement of primary chalcopyrite by covellite, and covellite by goethite (Fig. 6); the deposition of goethite as cavity filling between brecciated quartz and as rims along quartz grains and fine-grained chalcopyrite; and extensive chloritization of the host granulite complex. Further study with systematic samples, however, is recommended to understand whether the fluid responsible for secondary enrichment/remobilization arose from below or descended from the surface.

6 SUMMARY AND CONCLUSIONS

SelFrag proved to be an excellent rock fragmentation system to liberate sufficient gold/electrum grains without affecting the original size or deforming the original shape of the grains. As an adequate sample processing technology, the liberation process enables 3D investigation of gold/electrum grain surfaces with respect to structures, replacement and alteration. It was possible to determine an actual value for the mineral grain-size distribution, which could further be useful for ore process design and optimization. Hence, such a fragmentation system along with the consecutive preconcentration processes makes studies on the size, texture and morphology of gold/electrum and other related minerals possible. It offers nearly unprecedented opportunities to extract additional information on the formation, deposition and distribution of minerals, including gold and electrum as investigated here.

SEM-EDS analyses indicated that gold in the

present samples varied in composition from almost pure gold to a composite alloy containing significant amounts of Ag and traces of Cu, Fe and Hg. However, Au–Ag minerals mainly occurred as electrum. Associated minerals were acanthite along with electrum and chalcopyrite, well-developed crystals of iodargyrite, fine-grained silver and bismuth tellurides and native bismuth, as well as various types of rarely occurring sulphides. Studies on more samples should be conducted to conclude on the source of the gold/electrum. However, on the basis of the total mineral assemblage, the texture, grain morphology and chemical composition from the present samples, primary electrum/gold and pseudomorph acanthite (originally argentite) were deposited along with the pre-existing sulphides and partially remobilized by either late-stage low-temperature hydrothermal or supergene processes.

7 ACKNOWLEDGEMENTS

I would like to thank Mr Veikko Keinänen and Dr Olli Sarapää who provided the samples, Ahti Nissinen for his assistance with selFrag operation and Leena Järvinen, who performed the HMS and magnetic separation of the fragmented samples. I

am grateful to Dr Kari Kinnunen for his valuable suggestions. Special thanks to my colleagues Bo Johanson for his assistance with SEM, to Stefanie Lode for editing the manuscript, and to Dr Jukka Marmo for translating the abstract.

REFERENCES

- Andres, U. 1995.** Electrical disintegration of rocks. *Mineral Processing and Extractive Metallurgy Review* 14, 87–110.
- Andres, U., Timoshkin, I., Jiresting, J. & Stallknecht, H. 2000.** Liberation of valuable inclusions in ores and slags by electrical pulses. *Powder Technology* 114, 40–50.
- Bluhm, H., Frey, W., Giese, H., Hoppé, P., Schultheiß, C. & Sträßner, R. 2000.** Application of pulsed HV discharges to Material Fragmentation and recycling. *IEEE Transactions on Dielectric and Electrical Insulation* 7, 625–636.
- Boyle, D. R. 1997.** Iodargyrite as an indicator of arid climate conditions and its association with gold-bearing glacial tills of the Chibougamau – Chapais area, Quebec. *The Canadian Mineralogist* 35, 22–34.
- Cabri, L. C., Rudashevsky, N. S., Rudashevsky, V. N. & Gorkovetz, V. Y. 2008.** Study of native gold from the Luopensulo deposit (Kostomuksha area, Karelia, Russia) using a combination of electric pulse aggregation (EPD) and hydroseparation (HS). *Minerals Engineering* 21, 463–470.
- Chernet, T. 2006.** Preliminary observation on the heavy fractions of selFrag fragmented Kimberlite samples (P7-A1 and P7-B1). Geological Survey of Finland, Research Lab. for Div. of Ammann Schweiz AG. 7 p.
- Chernet, T. 2007.** Preliminary observation on the heavy fractions of selFrag fragmented Kimberlite samples (Dinosaur egg (Dino)). Geological Survey of Finland, Research Lab. for Div. of Ammann Schweiz AG, February. 10 p.
- Chernet, T., Laukkanen, J., Werner, S., Marmo, J., O’Brein, H. & Huhma, H. 2007.** Preliminary report on particle size distribution and mineral liberation study of crushed tonalite and diabase rock: Comparison on the efficiency of roller crusher and selFrag. Geological Survey of Finland, unpublished report CM19/2007/1. 28 p.
- Gnos, E., Kurz, D., Leya, I. & Eggenberger, U. 2007.** Electrodynamic disaggregation of geologic material. *Goldschmidt 2007*.
- Grondijs, H. F. & Schouten, C. 1931.** Polished thin sections of ore and rock, *Economic Geology* 26(3), 343–345.
- Humphries, D. W. 1992.** The preparation of thin sections of rocks, minerals and ceramics. *Royal Microscopical Society, Oxford Science Publications, Microscopy Handbooks* 24. 83 p.
- Hutchinson, C. S. 1997.** *Laboratory Handbook of Petrographic Techniques*. New York: John Wiley and Sons Inc.
- Keinänen, V., Lahti, I., Sarala, P. & Sarapää, O. 2010.** Gold exploration in the Laanila area in the years 2005–2009, Inari, Finland Lapland. Geological Survey of Finland, unpublished report M19/3831/2010/26. 20 p.
- Lastra, R. & Cabri, L. J. 2003.** Comparative liberation study by image analysis of Merensky reef samples comminuted by electric pulse disaggregation and by conventional crusher. In: Lorenzen, I. et al. (eds), *Proceedings of the XXII International Mineral Processing Congress* 1, 251–260.
- Reich, M., Palacios, C., Alvear, M., Cameron, E. M., Leybourne, M. I. & Deditius, A. 2009.** Iodine-rich waters involved in supergene enrichment of the Mantos de la Luna argentiferous copper deposit, Atacama Desert, Chile. *Min. Deposita* 44, 719–722.
- Sheets, R. W., Craig, J. R. & Bodnar, R. J. 1995.** Composition and occurrence of electrum at the Morning Star deposit, San Bernardino County, California: Evidence for remobilization of gold and silver. *The Canadian Mineralogist* 33, 137–151.
- Sillitoe, R. H. 2007.** Hypogene reinterpretation of supergene silver enrichment at Chañarcillo, Northern Chile. *Economic geology* 102(5), 777–781.

The SelFrag laboratory scale equipment adequately released gold, electrum and related ore minerals from quartz and goethite sampled from the mineralized Oiva dyke, northern Finland, with no visible effect on the original shape, surface morphology and size (distribution) of the liberated grains. This study has confirmed the value of high-voltage pulsed fragmentation technology for gold and related mineral grain characterization and actual mineral grain size determination as a powerful tool in interpreting complex local and regional gold mineralization. The ability to assess these and other parameters with negligible artifacts attributable to sample preparation can contribute to a better understanding of the depositional environment and paragenesis of deposits.